RESEARCH ARTICLE

DC Conductivity and Mobility of a Degenerate Electron Gas in Heavily Doped GaN Crystals at Room Temperature

Nikolai A. Poklonski[1] | Ilya I. Anikeev[1] | Evgenii V. Lutsenko[2] | Sergey A. Vyrko[1]

[1]Faculty of Physics, Belarusian State University, Minsk, Belarus | [2]Center for Wide-Band-Gap Nano- and Microelectronics, B.I. Stepanov Institute of Physics of the NAS of Belarus, Minsk, Belarus

Correspondence: Nikolai A. Poklonski (poklonski@bsu.by)

Received: 14 October 2025 | **Revised:** 22 November 2025 | **Accepted:** 3 December 2025

Keywords: electron mobility edge | electrostatic fluctuations | heavily doped semiconductor | n-type gallium nitride | room temperature

ABSTRACT

We consider *n*-type gallium nitride crystals heavily doped with hydrogen-like donors (silicon or germanium atoms) and weakly to moderately compensated by hydrogen-like acceptors (magnesium atoms). Donor and acceptor concentrations correspond to the metallic side of the insulator–metal concentration phase transition (Mott transition). The shift of the conduction band (CB) electron mobility edge into the bandgap, caused by electrostatic fluctuations in the interaction energy between electrons and impurity ions, is taken into account. Within the relaxation time approximation for electron quasi-momentum, the dependences of stationary (DC) electrical resistivity and drift mobility on the concentration of CB electrons in *n*-GaN crystals are calculated. Each act of elastic Coulomb scattering of a CB electron by a donor or acceptor ion is assumed to occur within a spherical volume of the crystal matrix associated with a single ion. Electron scattering on phonons is considered according to Matthiessen's rule. The calculation results, obtained using the proposed formulas without fitting parameters, quantitatively agree with experimental data over a wide range of CB electron concentrations. From analysis of experimental data, a new approximation formula for drift mobility at room temperature is obtained. The results using the new approximation and the proposed theoretical formula are consistent.

1 | Introduction

Crystalline III-nitrides (AlN, GaN, and InN) with a wurtzite structure and solid solutions based on them are direct-gap semiconductors with a bandgap from ≈6.2 eV for AlN to ≈3.4 eV for GaN and ≈0.7 eV for InN at room temperature [1], which provides the operation of optoelectronic devices from the deep ultraviolet to the near infrared region of the spectrum. The breakthrough in epitaxial growth and doping of GaN to *p*-type electrical conductivity in the early 1990s turned GaN into one of the most important materials for the semiconductor industry. The creation of the first blue light-emitting diodes (LEDs) [2] marked the beginning of the production of violet and blue laser diodes [3]. The production of white LEDs based on blue gallium nitride LED crystals and yellow phosphor [4] led to the "LED revolution" in lighting and the Nobel Prize in Physics 2014 [5]. Further improvement of technologies for the epitaxial growth of III-nitride layers led to the creation of green LEDs and lasers, LED and laser projectors, and micro-LED displays. Currently, research on ultraviolet LEDs [6], lasers [7], and photodetectors [8, 9] is relevant, and a new field is also developing—integrated photonics on a crystal [9, 10]. High breakdown electric field strengths (≈3.3 MV/cm [11]) and the piezoelectric properties of wurtzite, which allow the formation of two-dimensional electron or hole gas at III-nitride heterointerfaces [12] with high electron or hole concentration and mobility, serve as a basis for creating powerful field-effect transistors (see, e.g., refs. [13, 14]). Also, the design and manufacturing of high-frequency and power transistors with high electron mobility based on GaN are currently being developed (see, e.g., ref. [15]).

Despite the successes achieved, a drawback of III-nitride technologies is still the *p*-type electrical conductivity crystals, which have high electrical resistivity ρ_p (low conductivity $\sigma_p = 1/\rho_p$) and optical losses [16], making it difficult to increase the efficiency of light-emitting and laser diodes. Therefore, minimizing the thickness of the *p*-type layers through the use of piezoelectric doping and tunneling junctions is of particular importance. Meanwhile,

© 2026 Wiley-VCH GmbH.

the minimum internal electrical resistivity of light-emitting and laser diodes that emit in the visible region of the spectrum is ensured by the use of a transparent low-resistance heavily doped n^{++}-GaN with electron concentration $\approx 10^{20}\ \mathrm{cm}^{-3}$. The use of n^{++}-GaN in transistors for ultra-low-resistance non-annealed contact to two-dimensional electron gas [17] allows for low on-state losses in power transistors, high efficiency values, and high microwave cutoff frequencies [18].

Therefore, the description of the physical mechanisms of electrical conductivity and drift mobility of III-nitride semiconductor crystals, especially at high dopant concentrations, is a relevant task. Studying the relationship between defect concentration and electrical conductivity in III-nitride-based crystals will ensure reproducibility of characteristics and allow for the prediction of the durability and reliability of devices in aggressive environments, at high temperatures, and under high radiation backgrounds. Note that control of electrical conductivity is important in the design of III-nitride-based photodetectors [19]. In particular, high transmittance in the ultraviolet region of the spectrum and the possibility of forming two-dimensional electron gas open the way to the creation of ultrafast photonic devices and UV sensors [20].

The purpose of the work is to calculate the dependences of the stationary electrical resistivity and drift mobility on the conduction band (CB) electron concentration in heavily doped weakly and moderately compensated n-type gallium nitride crystals, taking into account the elastic scattering of mobile electrons by Coulomb potential created by hydrogen-like impurity ions at room temperature.

Note that the calculation results for the stationary electrical resistance and drift mobility can be used in the design and manufacturing of modern electronic and optoelectronic devices based on heavily doped GaN. Such devices include high-electron-mobility transistors (HEMTs) with ultra-low contact resistance, vertical power diodes and transistors, tunnel junctions in LED structures, as well as UV photodetectors with transparent conductive contacts. For example, during the development of power GaN transistors and microwave nanostructures (see, e.g., refs. [15, 21]), it is important to control the electrical resistivity and drift mobility: the higher the electron drift mobility value and the lower the doping impurity concentrations, the lower power loss and heat dissipation, which consequently leads to higher efficiency and operational stability under extreme conditions. From a manufacturing technology perspective, a deep understanding of the electrical conductivity mechanisms in III-nitrides allows for the development of more uniform and pure crystals, which can also ensure the reproducibility of device characteristics during large-scale production.

2 | Ionization Equilibrium of CB Electrons and Impurity Ions

Let us consider a heavily doped n-type semiconductor at room temperature, when all hydrogen-like impurities are ionized, and it is on the metallic side of the insulator–metal concentration phase transition (Mott transition [22]). The concentration of donors in the charge state $(+1)$ is equal to the total concentration of donors N, and the concentration of acceptors in the charge state (-1) is equal to the total concentration of acceptors KN, where $0<K<1$ is the degree of compensation of donors by acceptors. (The charge states of impurity ions are given in units of the elementary charge e.) The electrical neutrality in this case means that the total positive charge of the donor ions is equal to the total negative charge of all electrons and acceptor ions in the crystal and has the form

$$N = n + KN \tag{1}$$

where n is the average concentration of all electrons in the CB.

According to Equation (1), the number of electrons n can be obtained by subtracting the total number of acceptors KN from the total number of donors N, in the unit volume of the crystal, as $n=(1-K)N$.

From Equation (1), it follows that the concentration of all impurity ions $N_{\mathrm{ion}}=(1+K)N$ in the semiconductor is greater than the electron concentration n. The total concentration of point charged particles (donor ions, acceptor ions, and electrons with charge $\pm e$) in the semiconductor crystal is $N_{\mathrm{ch}}=n+N+KN=2N$.

In the three-dimensional n-type semiconductor, the density of single-electron states in a local region of the sample with an electron potential energy U is equal to [23]

$$g_{\mathrm{loc}}(E-U)=\frac{V(2m_{\mathrm{nd}})^{3/2}}{2\pi^2\hbar^3}(E-U)^{1/2} \tag{2}$$

where V is the volume of the crystalline sample; $m_{\mathrm{nd}}=\nu^{2/3}m_{nd}^{(1)}$ is the density-of-states effective mass of electrons in the CB; ν is the number of valleys (equivalent electron energy minima in the CB; $\nu=1$ for n-GaN); $m_{\mathrm{nd}}^{(1)}$ is the density-of-states effective mass in one valley; E is the total energy of the electron; $E_{\mathrm{kin}}=E-U$ is the kinetic energy of CB electron; and $\hbar=h/2\pi$ is the reduced Planck constant.

The average over the crystalline sample density of single-electron states in the CB, taking into account fluctuations of the electrostatic potential energy ($W_n\neq 0$ and $E_{\mathrm{m}}^{(c)}\neq E_c=0$; see Figure 1), is given by [24, 25]

$$\begin{aligned} g_{\mathrm{av}}(E) &= \int_{-\infty}^{E} g_{\mathrm{loc}}(E-U)\,\mathcal{G}(U)\,\mathrm{d}U \\ &= V\frac{(2m_{\mathrm{nd}})^{3/2}}{2\pi^2\hbar^3}\int_{-\infty}^{E}(E-U)^{1/2}\,\mathcal{G}(U)\,\mathrm{d}U \end{aligned} \tag{3}$$

where $g_{\mathrm{loc}}(E-U)$ is given by Equation (2), and $\mathcal{G}(U)$ is the distribution density of potential energy fluctuations of an electron over the crystalline sample.

Note that the formation of $g_{\mathrm{av}}(E)$ on the metallic side of the Mott transition for a crystalline n-type semiconductor is due to the hybridization of the wave functions of electrons on donors and the Bloch wave functions of CB electrons [26].

Then the average over the sample volume V electron concentration in the CB (at the complete ionization of hydrogen-like impurity atoms) is equal to

$$n=\frac{1}{V}\int_{-\infty}^{+\infty} g_{\mathrm{av}}(E)f_n(E)\,\mathrm{d}E=(1-K)N \tag{4}$$

where $f_n(E)=\{1+\exp[(E-E_{\mathrm{F}}^{(c)})/k_{\mathrm{B}}T]\}^{-1}$ is the Fermi–Dirac distribution function, $E_{\mathrm{F}}^{(c)}$ is the Fermi level (measured from

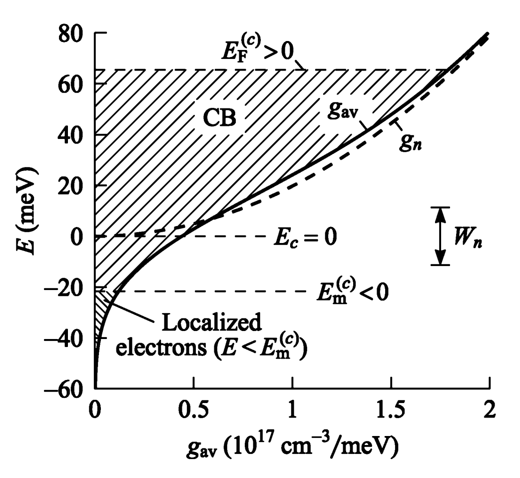

FIGURE 1 | Energy band diagram (plot of the single-electron energy E as a function of the density of states g_{av} shown by a solid line; cf. diagrams from refs. [24, 25]) of a doped n-GaN with electron concentration $n = 1 \times 10^{19}$ cm^{-3} and compensation ratio $K = 0.03$ at room temperature ($T = 300$ K) calculated using Equation (3), taking into account the effective mass of electrons m_{nd} according to Equation (19). The bottom of the conduction band (CB) of an undoped (ideal) crystal ($E_c = 0$) is set as the reference point of the electron energy E; $E_F^{(c)} > 0$ is the Fermi level determined from the solution of Equation (4) (electron-filled states are shaded: localized states—left shading, mobile states—right shading); $E_m^{(c)} < 0$ is the drift mobility edge for the CB electrons given by Equation (10); g_n (dashed line) is the density of states in the CB of an undoped n-GaN crystal calculated using Equation (13); $g_{av} \to g_n$ at $W_n \ll k_B T$; W_n is the root–mean-square fluctuation of the CB electron potential energy according to Equation (7); $k_B T$ is the thermal energy.

$E_c = 0$), k_B is the Boltzmann constant, and T is the absolute temperature.

Further, following refs. [23, 27], we assume that the distribution density of the potential energy fluctuations of an electron over the volume of the crystalline sample has a Gaussian (normal) form

$$\mathcal{G}(U) = \frac{1}{\sqrt{2\pi}W_n} \exp\left[-\left(\frac{U}{\sqrt{2}W_n}\right)^2\right] \quad (5)$$

where W_n is the root–mean-square (rms) fluctuation of the CB electron energy (Figure 1).

Taking into account the Coulomb interaction of only the nearest point charged particles the rms fluctuation W_d of the electrostatic energy of an immobile impurity ion is [27, 28]

$$W_d \approx 2.64 \frac{e^2}{4\pi\varepsilon} N_{ch}^{1/3} \quad (6)$$

where e is the elementary charge; $\varepsilon = \varepsilon_r \varepsilon_0$ is the absolute static permittivity of the crystalline semiconductor, ε_r is the relative permittivity due to valence band (VB) electrons of the crystal matrix, ε_0 is the electric constant, and $N_{ch} = n + KN + N = 2N$ is the concentration of all point charged particles and quasiparticles (impurity ions and CB electrons), which satisfies the electrical neutrality (4) of the crystal. (Under this condition, the average over the crystalline sample potential energy of the Coulomb interaction of the nearest donor ions, acceptor ions, and CB electrons is zero [24]).

The value of W_n at $n = (1-K)N$ is given by the expression [27, 29]

$$W_n \approx 0.29 \left(\frac{n}{N_{ch}}\right)^{1/2} W_d = 0.21(1-K)^{1/2} W_d \quad (7)$$

The quantity W_d, given by Equation (6), describes the rms fluctuation of the electrostatic potential energy created by immobile impurity ions randomly (Poissonian) distributed over the crystal volume. However, the CB electron is capable of partially screening this disorder. This is due to the fact that electrostatic fluctuations on scales smaller than the average de Broglie wavelength of a free electron do not manifest themselves and, consequently, the quantity W_n turns out to be less than W_d. Equation (7) quantitatively expresses this relation. The significance of the quantity W_n lies in its ability to account for the tails of the single-electron density of states g_{av} (Figure 1) when determining the Fermi level $E_F^{(c)}$ by solving the electrical neutrality Equation (4), as well as the contribution of these tails to the electrical conductivity and drift mobility of CB electrons.

Note that the average de Broglie wavelength of CB electrons increases with decreasing electron concentration, so that at low electron concentrations they "do not notice" the nearest point charged particles [24, 27]. This physical mechanism is reflected in Equation (7): as the value of $W_n \to 0$ when the compensation ratio $K \to 1$, which corresponds to the electron concentration $n \to 0$.

The concentration n_m of mobile electrons in the CB with the total energy $E = E_{kin} + U$ exceeding the drift-diffusion mobility edge $E_m^{(c)}$ (see Figure 1), required for their migration throughout the entire volume of three-dimensional semiconductor crystal, is determined from Equation (4) and is given by

$$\begin{aligned} n_m &= \frac{1}{V} \int_{E_m^{(c)}}^{\infty} f_n g_{av}(E)\, dE \\ &= \frac{(2m_{nd})^{3/2}}{2\pi^2\hbar^3} \int_{E_m^{(c)}}^{\infty} f_n \int_{-\infty}^{E} \sqrt{E-U}\, \mathcal{G}(U)\, dU\, dE = n - n_l \end{aligned} \quad (8)$$

where $n = (1-K)N$; the concentration of electrons n_l that can migrate only in limited regions of the sample (at $E < E_m^{(c)}$) is

$$n_l = \frac{(2m_{nd})^{3/2}}{2\pi^2\hbar^3} \int_{-\infty}^{E_m^{(c)}} f_n \int_{-\infty}^{E} \sqrt{E-U}\, \mathcal{G}(U)\, dU\, dE \quad (9)$$

The mobility edge for CB electrons [25] is equal to [30, 31]

$$E_m^{(c)} \approx -0.955 W_n < 0 \quad (10)$$

where the value of W_n is determined by Equation (7) taking into account Equation (6).

3 | Model of Conductivity and Drift Mobility of Electrons at Their Elastic Scattering by Impurity Ions

According to ref. [31], in the single-electron approximation for the DC electrical conductivity σ_{ion} of an n-type semiconductor, taking into account Equation (3)–(10), we have

$$\sigma_{\text{ion}} = \frac{e^2}{m_{n\sigma}} \frac{(2m_{\text{nd}})^{3/2}}{3\pi^2\hbar^3} \int_{E_{\text{m}}^{(c)}}^{\infty} \frac{f_n(1-f_n)}{k_{\text{B}}T} \int_{-\infty}^{E} \tau_{\text{ion}}(E-U) \times (E-U)^{3/2}\,\mathcal{G}(U)\,\mathrm{d}U\,\mathrm{d}E \tag{11}$$

where $m_{n\sigma}$ is the electrical conductivity effective mass of an electron; $\tau_{\text{ion}}(E-U)$ is the quasi-momentum relaxation time of an electron (with the kinetic energy $E_{\text{kin}} = E-U$); and $f_n(1-f_n) = \{4\cosh^2[(E-E_{\text{F}}^{(c)})/2k_{\text{B}}T]\}^{-1}$.

It is assumed that the acts of elastic Coulomb scattering of a CB electron by impurity ions are independent incompatible events. In the Born approximation [32], the quasi-momentum relaxation time of an electron with the kinetic energy $E_{\text{kin}} = E-U > 0$ (at $E > E_{\text{m}}^{(c)}$) included in Equation (11) during elastic scattering by ions of hydrogen-like impurities in the crystal matrix is [33, 34]

$$\tau_{\text{ion}}(E-U) = \left(\frac{4\pi}{3}\right)^{1/3} \left(\frac{4\pi\varepsilon}{e^2}\right)^2 \frac{\hbar}{N_{\text{ion}}^{2/3}}(E-U) \times \left\{\ln\left[1 + \left(\frac{8\pi\varepsilon R_{\text{ion}}(E-U)}{e^2}\right)^2\right]\right\}^{-1} \tag{12}$$

where $N_{\text{ion}} = (1+K)N = (1+K)n/(1-K)$ is the concentration of electron-scattering impurity ions; $R_{\text{ion}} = [3/(4\pi N_{\text{ion}})]^{1/3} \approx 0.62N_{\text{ion}}^{-1/3}$ is the radius of a spherical region in a crystal matrix associated with each impurity ion, within which a single electron scattering event occurs due to the Coulomb field of that impurity ion; function $\ln(\cdot)$ denotes the natural logarithm. Note that when deriving Equation (12), only the Coulomb interaction of an electron with an impurity ion located in the center of a sphere with a volume of $1/N_{\text{ion}}$ was taken into account. It was assumed that the local static relative permittivity of the crystal matrix ε_{r} in the vicinity of each impurity ion is determined by VB electrons.

Note that neglecting the electrostatic fluctuations of the potential energy of electrons ($W_n \ll k_{\text{B}}T$), when $\mathcal{G}(U) \to \delta(U)$, we have $E_{\text{m}}^{(c)} \to E_c$ (see Figure 1), and then according to Equation (8) we have $n_l \to 0$ and $n_{\text{m}} \gg n_l$, where $\delta(U)$ is the Dirac delta function. The inequality $n_{\text{m}} \gg n_l$ justifies the use of the total CB electron concentration n in Equation (7), rather than the concentration of mobile electrons n_{m}. In this case, the density of single-electron states in the CB according to Equation (3) transforms into the standard formula for a lightly doped crystalline semiconductor:

$$g_{\text{av}} \to g_n = V\frac{(2m_{\text{nd}})^{3/2}}{2\pi^2\hbar^3}\sqrt{E_{\text{kin}}} \tag{13}$$

The static electrical conductivity σ_{ion} according to Equation (11) transforms into the standard formula for electrical conductivity without taking into account fluctuations [35–37], and for Equation (12) we have $\tau_{\text{ion}}(E-U) \to \tau_{\text{ion}}(E)$ at $E_{\text{kin}} = E$.

The Fermi level $E_{\text{F}}^{(c)}$ is found from the solution of the electrical neutrality Equation (4). In numerical calculations, it is convenient to choose the approximation $E_{\text{F}}^{(c)} = \zeta_{\text{F}}^{(c)}[1-(\pi^2/12)(k_{\text{B}}T/\zeta_{\text{F}}^{(c)})^2]$ as the initial value for $E_{\text{F}}^{(c)} > 3k_{\text{B}}T$, which is the chemical potential of electrons [28, 37, 38], where $\zeta_{\text{F}}^{(c)} = (\hbar^2/2m_{\text{nd}})(3\pi^2 n)^{2/3}$ is the Fermi energy of degenerate electron gas; $E_{\text{F}}^{(c)} \to \zeta_{\text{F}}^{(c)}$ at $T \to 0$.

We assume that the scattering by phonons of the crystal structure does not depend on the electrostatic fluctuations of potential energy, given by Equation (7), i.e., $\mathcal{G}(U) \to \delta(U)$. Then the stationary electrical conductivity of the semiconductor, caused by scattering of mobile electrons with the concentration n_{m} on the crystal lattice vibrations, is

$$\sigma_{\text{lat}} = e n_{\text{m}} \mu_{\text{lat}} \tag{14}$$

where μ_{lat} is the drift mobility of CB electrons due to their scattering on phonons of the crystal matrix.

According to Matthiessen's rule, the total DC electrical conductivity of the semiconductor σ_n has the form [35, 36]

$$\frac{1}{\sigma_n} \equiv \rho_n = \frac{1}{\sigma_{\text{ion}}} + \frac{1}{\sigma_{\text{lat}}} \tag{15}$$

where ρ_n is the electrical resistivity of the semiconductor; σ_{ion} is given by Equation (11); and σ_{lat} is given by Equation (14).

The drift mobility of CB electrons, limited by their elastic scattering on impurity ions in an n-type semiconductor, is determined as follows

$$\mu_{\text{ion}} = \frac{\sigma_{\text{ion}}}{e n_{\text{m}}} \tag{16}$$

where σ_{ion} is determined by Equation (11) taking into account Equation (12), and n_{m} is determined by Equation (8).

The total drift mobility of electrons μ_n, similar to Equation (15), is determined according to Matthiessen's rule

$$\frac{1}{\mu_n} = \frac{1}{\mu_{\text{ion}}} + \frac{1}{\mu_{\text{lat}}} \tag{17}$$

The quasi-wave vector $k_n(E_{\text{kin}})$ of a CB electron in the region with potential energy U and kinetic energy $E_{\text{kin}} = E-U$ is $k_n(E-U) = \sqrt{2m_{nd}(E-U)}/\hbar$. Then for the average value of the quasi-wave vector of a mobile CB electron, we derive

$$\begin{aligned}\langle k_n \rangle &= \frac{1}{n_{\text{m}}V} \int_{E_{\text{m}}^{(c)}}^{\infty} f_n \int_{-\infty}^{E} g_{\text{loc}}(E-U)\,k_n(E-U)\mathcal{G}(U)\,\mathrm{d}U\,\mathrm{d}E \\ &= \frac{1}{n_{\text{m}}} \frac{(2m_{nd})^{5/2}}{2\pi^2\hbar^4} \int_{E_{\text{m}}^{(c)}}^{\infty} f_n \int_{-\infty}^{E} (E-U)\,\mathcal{G}(U)\,\mathrm{d}U\,\mathrm{d}E\end{aligned} \tag{18}$$

where $g_{\text{loc}}(E-U)$, n_{m} and $E_{\text{m}}^{(c)}$ are given by Equations (2), (8), and (10), respectively.

Note that Ge and Si atoms, substituting Ga atoms in the crystal structure of GaN on the insulator side of the Mott transition, are hydrogen-like donors. On the metallic side of the Mott transition, these impurities can substitute nitrogen atoms in the crystal structure of GaN, becoming hydrogen-like acceptors. This phenomenon in binary semiconductors, such as GaAs, ZnO, Cu_2O, etc., is known as impurity self-compensation [39, 40, 41]. Consequently, the compensation ratio can increase with increasing impurity concentration.

4 | Comparison of Calculation Results with Experimental Data and Discussion

To compare the calculation results of DC electrical resistivity $\rho_n = 1/\sigma_n$ with experimental data, heavily doped n-type gallium nitride crystals with degrees of compensation $K \leq 0.7$ of donors

(silicon or germanium atoms) by acceptors (magnesium atoms) were chosen. For n-GaN:Si crystals, the donor concentration N was greater than the Mott concentration $N_M \approx 1.6 \times 10^{18}$ cm^{-3} at $K \leq 0.01$ (experimental value from ref. [42]), which finds calculation support [43]. Experimental values N_M for n-GaN:Ge are not yet available in the literature.

The following physical values are used in calculations of the stationary electrical resistivity in gallium nitride crystals [1, 11, 44]: (number of valleys in the CB $\nu = 1$) $\varepsilon_r = 9.5$, $\mu_{lat} = 900$ cm^2/V·s; $m_{nd} = m_{n\sigma} = 0.22 m_0$, where m_0 is the electron mass in vacuum.

Note that for the considered range of CB electron concentrations 1×10^{19} cm$^{-3} \leq n \leq 1 \times 10^{21}$ cm^{-3}, the rms fluctuation W_n of the CB electron energy according to Equation (7) increases $\propto n^{1/3}$ from 22.8 to 105.6 meV for $K = 0.01$ and from 18.7 to 86.6 meV for $K = 0.7$.

Figure 2 shows the experimental and calculated dependences of the DC electrical resistivity $\rho_n = 1/\sigma_n$ on the CB electron concentration. Weakly and moderately compensated ($K \leq 0.7$) n-GaN crystals at an absolute temperature $T \approx 300$ K are considered. The curves are calculation of $\rho_n \equiv 1/\sigma_n$ using Equation (15), taking into account fluctuations W_n for $K = 0.01$ (curve *1*) and $K = 0.7$ (curve *2*). Experimental data for n-GaN:Ge (*a*) and n-GaN:Si (*b*, *c*) are shown: data (*a*, *b*) from refs. [45–65], (*c*) from ref. [66].

Figure 3 shows the experimental and calculated dependences of the Hall (experiment) and drift (calculation) mobilities on the CB electron concentration. Weakly and moderately compensated ($K \leq 0.7$) n-GaN crystals at an absolute temperature $T \approx 300$ K are considered. The solid curves are calculation of μ_n using Equation (17), taking into account fluctuations W_n for $K = 0.01$ (curve *1*) and $K = 0.7$ (curve *2*); the dashed curves *1′* and *2′* are calculation of μ_n using the approximation Equation (20) from ref. [66] for $K = 0.01$ (curve *1′*) and $K = 0.7$ (curve *2′*); and the dashed curves *1″* and *2″* are calculation of μ_n using the approximation Equation (21) for $K = 0.01$ (curve *1″*) and $K = 0.7$ (curve *2″*). Experimental data for n-GaN:Ge (*a*) and n-GaN:Si (*b*, *c*) are shown: data (*a*, *b*) from refs. [45–65].

For n-GaN crystals ($\nu = 1$; $\varepsilon_r = 9.5$), it is necessary to take into account the dependence of the effective masses of CB electrons $m_{nd} = m_{n\sigma}$ on their concentration. Approximating the experimental data collected in refs. [11, 44], we obtain

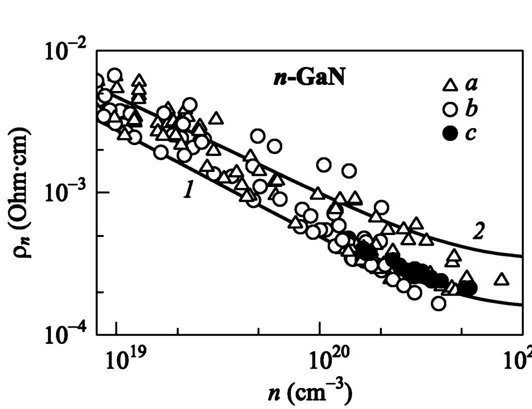

FIGURE 2 | DC electrical resistivity $\rho_n = 1/\sigma_n$ of an n-type gallium nitride as a function of the CB electron concentration n at $T \approx 300$ K. Points are the experimental data on: n-GaN:Ge (*a*), n-GaN:Si (*b*) from refs. [45–65], and n-GaN:Si (*c*) from ref. [66]; lines are the calculations according to Equation (15): $K = 0.01$ (curve *1*); $K = 0.7$ (curve *2*).

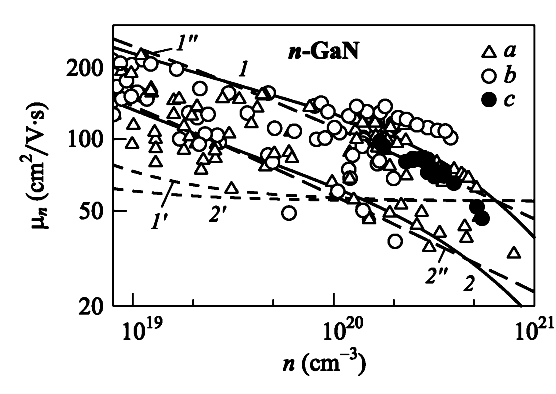

FIGURE 3 | Drift mobility μ_n of electrons in an n-type gallium nitride as a function of the CB electron concentration n at $T \approx 300$ K. Points are the Hall mobility measurement data on: n-GaN:Ge (*a*), n-GaN:Si (*b*) from refs. [45–65], and n-GaN:Si (*c*) from ref. [66]; lines are the calculations for $K = 0.01$ (curves *1*, *1′*, and *1″*) and $K = 0.7$ (curves *2*, *2′*, and *2″*): solid lines *1* and *2*—using Equation (17), dashed lines *1′* and *2′*—using the approximation Equation (20) from ref. [67], and dashed lines *1″* and *2″*—using the approximation Equation (21).

$$m_{nd}(n) = m_{n\sigma}(n) = m_{nd}[1 + 0.09(n/n_*)^{1.04}] \quad (19)$$

where $m_{nd} = m_{n\sigma} = 0.22 m_0$, $n_* = 1 \times 10^{20}$ cm^{-3} is the fitting parameter.

In ref. [67], an analytical approximation of the dependence of the CB electron mobility in n-GaN on the concentration of hydrogen-like donors is given. For the temperature $T = 300$ K, this approximation has the form

$$\mu_n(N) = \frac{\mu_{max} + (N/N_g)\mu_{min}}{1 + (N/N_g)} \quad (20)$$

where $N = n/(1-K)$ is the concentration of completely ionized donors; $\mu_{max} = 1000$ cm^2/V·s and $\mu_{min} = 55$ cm^2/V·s are the electron mobilities in lightly doped and heavily doped n-type gallium nitride samples, respectively; and $N_g = 2 \times 10^{17}$ cm^{-3} is the fitting parameter. From Figure 3 (curves *1′*, *2′*), it is clear that the approximation using Equation (20) does not fully describe the decrease in the mobility value with an increase in the CB electron concentration and the compensation of donors by acceptors. This is due to the following factors: (i) Equation (20) was derived based on experimental data that were limited in the range of electron concentrations (up to 10^{18} cm^{-3}). These data did not include systematic measurements for samples with high doping levels at reliably established compensation ratios, which significantly limits its applicability in practice. (ii) The experimental data used to validate Equation (20) were obtained on GaN crystals that had a less perfect crystal structure (higher defect concentration) compared to modern samples.

Instead of approximation Equation (20), we propose the following approximation for electron mobility μ_n (in the ranges 1×10^{19} cm$^{-3} \leq n \leq 1 \times 10^{21}$ cm^{-3} and $0.01 \leq K \leq 0.7$)

$$\mu_n(n, K, T_i) = \frac{\mu_{lat}(T_i)}{1 + (1+K)^{1.4}(n/n_g)^{0.42}} \quad (21)$$

where T_i is the temperature at which all donors are ionized and the CB electron concentration $n = (1-K)N$; $\mu_{lat}(T_i) = 900$ cm^2/V·s at $T_i = 300$ K; $n_g = 1 \times 10^{18}$ cm^{-3} is the fitting parameter.

The results of calculations using Equation (21) are shown by curves *1″* and *2″* in Figure 3, and they practically coincide with the results of calculations using the proposed theoretical Equation (17), shown by curves *1* and *2*. Note that the modern experimental data (Figure 3), from which approximation Equation (21) was obtained, are more extensive and systematic, making it possible to identify discrepancies that were not apparent when Equation (20) was derived based on a less complete set of data. The justification for obtaining approximation Equation (21) is a regression analysis of modern extensive experimental data, as well as the necessity to take into account the explicit dependence of the drift mobility μ_n on the compensation ratio K, which is absent in Equation (20). The functional form $1/[1+(1+K)^{1.4}(n/n_g)^{0.42}]$ is chosen as the simplest, physically motivated model, which takes into account the decrease in the value of drift mobility μ_n with an increase in the electron concentration n and the compensation ratio K. Parameters 1.4 and 0.42 are obtained by least squares fitting for the best correspondence to the experimental dataset in the ranges 1×10^{19} cm$^{-3} \le n \le 1\times10^{21}$ cm^{-3} and $0.01 \le K \le 0.7$.

From Figures 2 and 3, it is evident that, in general, there is agreement between the calculations using the proposed Equations (11)–(17) and the experimental data for n-GaN crystals on the metallic side of the Mott transition.

Note that the calculation of the electron quasi-momentum relaxation time using Equation (12), taking into account the diameter $2R_{\text{ion}} \approx 1.24N_{\text{ion}}^{-1/3}$ of a spherical region associated with an impurity ion, was performed in the Born approximation. The condition for the applicability of the Born approximation [32–34] has the form: $2\langle k_n\rangle R_{\text{ion}} > 1$, where $\langle k_n\rangle$ is given by Equation (18). The value $2\langle k_n\rangle R_{\text{ion}}$ decreases from 3.5 to 2.9 for $K=0.01$ and from 2 to 1.6 for $K=0.7$ with an increase in the concentration of delocalized CB electrons $n_{\text{m}} \approx n = (1-K)N$ from 10^{19} to 10^{21} cm^{-3}, i.e., the calculation of the electron drift mobility using Equation (16) is correct. It is also taken into account that $n_{\text{m}} \gg n_l$.

Note that some discrepancy between the calculated curves [68] and the experimental data may be due to the fact that in a number of experimental works, the value of the Hall factor was not taken into account for determining the CB electron concentration when processing data from Hall effect measurements for n-GaN. Also, in a number of works, the compensation of donors by acceptors in the crystals was not controlled. In this work, we did not consider the scattering of CB electrons by "donor ion–acceptor ion" pairs [69], as well as by small (compared to the average de Broglie wavelength of CB electrons) isolated clusters of several donor ions [70, 71]. Here, we note that the works [69–71] are based on the Brooks–Herring model, which uses a screened Coulomb potential. However, this potential, in contrast to the purely Coulomb potential, is not the potential for the pair interaction "CB electron–impurity ion" (see refs. [33, 34] and references therein).

5 | Conclusions

Within the framework of the Born approximation, the model of the elastic scattering of CB electrons by immobile hydrogen-like impurity ions (both donors and acceptors) in heavily doped degenerate n-GaN crystals located on the metallic side of the Mott transition is developed. It is assumed that a single act of elastic Coulomb scattering of an electron by an ion occurs during the time of its flight throught a spherical region (with radius $R_{\text{ion}} = [3/(4\pi N_{\text{ion}})]^{1/3} \approx 0.62N_{\text{ion}}^{-1/3}$) associated with an impurity ion in the crystal matrix at their total concentration $N_{\text{ion}} = (1+K)N$, where N is the concentration of completely ionized donors, and KN is the concentration of acceptors that compensate donors. The shift of the drift-diffusion mobility edge of CB electrons deep into the energy bandgap, due to the electrostatic fluctuations of their potential energy, is taken into account. The Matthiessen's rule takes into account the electron mobility limited by their scattering on phonons. The calculation results using the proposed formulas are in numerical agreement with known experimental data for n-GaN:Si and n-GaN:Ge at the CB electron concentration 1×10^{19} cm$^{-3} \le n = (1-K)N \le 1\times10^{21}$ cm^{-3} for weak ($K \le 0.01$) and moderate ($K \le 0.7$) compensations of donors (germanium or silicon atoms) by acceptors.

Acknowledgments

This study was supported by the Belarusian National Research Programs "Modern Materials Science, Advanced Materials, and New Technologies" and "Photonics and Microelectronics".

Funding

This study was supported by Ministry of Education of the Republic of Belarus (Belarusian National Research Program "Modern Materials Science, Advanced Materials, and New Technologies") and by the National Academy of Sciences of Belarus (Belarusian National Research Program "Photonics and Microelectronics").

Conflicts of Interest

The authors declare no conflicts of interest.

Data Availability Statement

The data that support the findings of this study are openly available in Mendeley Data at https://doi.org/10.17632/j956pswzz4, reference number [68].

References

1. I. Vurgaftman and J. R. Meyer, "Band Parameters for Nitrogen-Containing Semiconductors," *Journal of Applied Physics* 94 (2003): 3675.

2. S. Nakamura, T. Mukai, and M. Senoh, "High-Power GaN P-N Junction Blue-Light-Emitting Diodes," *Japanese Journal of Applied Physics* 30 (1991): L1998.

3. A. Khan, K. Balakrishnan, and T. Katona, "Ultraviolet Light-Emitting Diodes Based on Group Three Nitrides," *Nature Photonics* 2 (2008): 77.

4. J. Cho, J. H. Park, J. K. Kim, and E. F. Schubert, "White Light-Emitting Diodes: History, Progress, and Future," *Laser Photonics Reviews* 11 (2017): 1600147.

5. S. Nakamura, "Nobel Lecture: Background Story of the Invention of Efficient Blue InGaN Light Emitting Diodes," *Reviews of Modern Physics* 87 (2015): 1139.

6. J. Lang, F. Xu, J. Wang, et al., "Progress in Performance of AlGaN-Based Ultraviolet Light Emitting Diodes," *Advanced Electronic Materials* 11 (2025): 2300840.

7. H. U. Rehman, W. Bi, N. U. Rahman, et al., "A Review of Challenges, Solutions, and Improvements in the Performance of Deep Ultraviolet Semiconductor Laser Diodes (DUV LDs)," *ACS Applied Electronic Materials* 6 (2024): 8710.

8. R. Zhang, G. Wang, Q. Zhang, et al., "Recent Progress in GaN-Based Ultraviolet Photodetectors," *Journal of Materials Chemistry C* 13 (2025): 10972.

9. A. N. Semenov, D. V. Nechaev, D. S. Burenina, et al., "Solar-Blind Schottky Photodiodes Based on the AlGaN:Si/AlN Heterostructures Grown by Plasma-Activated Molecular Beam Epitaxy," *Technical Physics Letters* 50 (2024): 64.

10. S. Gündoğdu, S. Pazzagli, T. Pregnolato, et al., "AlGaN/AlN Heterostructures: an Emerging Platform for Integrated Photonics," *npj Nanophotonics* 2 (2025): 2.

11. S. Adachi, Properties of Semiconductor Alloys: Group-IV, III–V and II–VI Semiconductors (Wiley, 2009).

12. X. Liu, A. W. Bruch, and H. X. Tang, "Aluminum Nitride Photonic Integrated Circuits: from Piezo-Optomechanics to Nonlinear Optics," *Advances in Optics and Photonics* 15 (2023): 236.

13. C.-T. Ma and Z.-H. Gu, "Review of GaN HEMT Applications in Power Converters over 500 W," *Electronics* 8 (2019): 1401.

14. K. Husna Hamza and D. Nirmal, "A Review of GaN HEMT Broadband Power Amplifiers," *AEU-International Journal of Electronics and Communications* 116 (2020): 153040.

15. C. Li, X. Chen, and Z. Wang, "Review of the AlGaN/GaN High-Electron-Mobility Transistor-Based Biosensors: Structure, Mechanisms, and Applications," *Micromachines* 15 (2024): 00330.

16. S. W. Hamdy, S. P. DenBaars, J. S. Speck, and S. Nakamura, "Designs for III-Nitride Edge-Emitting Laser Diodes with Tunnel Junction Contacts for Low Internal Optical Absorption Loss," *Optical Engineering* 61 (2022): 027102.

17. H. Qie, J. Liu, Q. Li, et al., "Selective Area Epitaxy of Degenerate n-GaN for HEMT Ohmic Contact by MOCVD," *Applied Physics Letters* 121 (2022): 212106.

18. M. Micovic, D. Brown, D. Regan, et al., "Ka-Band LNA MMIC's Realized in $f_{\max} > 580$ GHz GaN HEMT Technology," *2016 IEEE Compound Semiconductor Integrated Circuit Symposium (CSICS)* (IEEE, 2016), 62–65.

19. T. V. Malin, A. M. Gilinskii, V. G. Mansurov, et al., "MBE-Grown AlGaN/GaN Heterostructures for UV Photodetectors," *Technical Physics* 60 (2015): 546.

20. Z. Lin, T. Lin, T. Lin, et al., "Ultrafast Response Self-Powered UV Photodetectors Based on GaS/GaN Heterojunctions," *Applied Physics Letters* 122 (2023): 131101.

21. N. V. Vostokov, M. N. Drozdov, M. A. Kalinnikov, S. A. Kraev, D. N. Lobanov, and P. A. Yunin, "Schottky Diodes Based on Monocrystalline Al/AlGaN/GaN Heterostructures for Zero-Bias Microwave Detection," *Technical Physics* 70 (2025): 1080.

22. N. F. Mott, *Metal–Insulator Transitions* (Taylor & Francis, 1990).

23. E. O. Kane, "Band Tails in Semiconductors," *Solid-State Electronics* 28 (1985): 3.

24. J. M. Ziman, *Models of Disorder: The Theoretical Physics of Homogeneously Disorded Systems* (Cambridge Univ. Press, 1979).

25. B. I. Shklovskii and A. L. Efros, *Electronic Properties of Doped Semiconductors* (Springer, 1984).

26. F. Gebhard, *The Mott Metal-Insulator Transition: Models and Methods* (Springer, 1997).

27. N. A. Poklonski, S. A. Vyrko, O. N. Poklonskaya, and A. G. Zabrodskii, "Role of Electrostatic Fluctuations in Doped Semiconductors upon the Transition from Band to Hopping Conduction (by the Example of *p*-Ge:Ga)," *Semiconductors* 50 (2016): 722.

28. N. A. Poklonskii and S. A. Vyrko, "Electrostatic Model of Edge Luminescence of Heavily Doped Degenerate Semiconductors," *Journal of Applied Spectroscopy* 69 (2002): 434.

29. N. A. Poklonski, S. A. Vyrko, O. N. Poklonskaya, A. I. Kovalev, and A. G. Zabrodskii, "Ionization Equilibrium at the Transition from Valence-Band to Acceptor-Band Migration of Holes in Boron-Doped Diamond," *Journal of Applied Physics* 119 (2016): 245701.

30. N. Mott, "The mobility edge since 1967," *Journal of Physics C: Solid State Physics* 20 (1987): 3075.

31. N. A. Poklonski, S. A. Vyrko, and A. N. Dzeraviaha, "Quasi-Classical Model of the Static Electrical Conductivity of Heavily Doped Degenerate Semiconductors at Low Temperatures," *Semiconductors* 52 (2018): 692.

32. A. Messiah, *Quantum Mechanics*. Chapter 19 (Dover, 2014).

33. N. A. Poklonski, S. A. Vyrko, V. I. Yatskevich, and A. A. Kocherzhenko, "A Semiclassical Approach to Coulomb Scattering of Conduction Electrons on Ionized Impurities in Nondegenerate Semiconductors," *Journal of Applied Physics* 93 (2003): 9749.

34. N. A. Poklonski, A. A. Kocherzhenko, S. A. Vyrko, and A. T. Vlassov, "A Comparison of Two-Particle Models for Conduction Electron Scattering on Hydrogen-Like Impurity Ions in Non-Degenerate Semiconductors," *Physica Status Solidi B* 244 (2007): 3703.

35. D. Jena, *Quantum Physics of Semiconductor Materials and Devices* (Oxford University Press, 2022).

36. K. Seeger, *Semiconductor Physics: An Introduction* (Springer, 2004).

37. N. W. Ashcroft and N. D. Mermin, *Solid State Physics* (Harcourt College Publishers, 1976).

38. B. M. Askerov, *Electron Transport Phenomena in Semiconductors* (World Scientific, 1994).

39. N. V. Agrinskaya and T. V. Mashovets, "Self-Compensation in Semiconductors: a Review Dedicated to the Hundredth Anniversary of the Birthday of Yakov Il'ich Frenkel'," *Semiconductors* 28 (1994): 843. [*Fiz. Tekh. Poluprovodn.* 28 (1994): 1505].

40. V. I. Fistul, *Impurities in Semiconductors: Solubility, Migration, and Interactions* (CRC Press, 2004).

41. Y. Tsur and I. Riess, "Self-Compensation in Semiconductors," *Physical Review B* 60 (1999): 8138.

42. A. Wolos, Z. Wilamowski, M. Piersa, et al., "Properties of Metal-Insulator Transition and Electron Spin Relaxation in GaN:Si," *Physical Review B* 83 (2011): 165206.

43. N. A. Poklonski, S. A. Vyrko, and A. G. Zabrodskii, "Electrostatic Models of Insulator–Metal and Metal–Insulator Concentration Phase Transitions in Ge and Si Crystals Doped by Hydrogen-Like Impurities," *Physics Solid State* 46 (2004): 1101.

44. O. Madelung, *Semiconductors: Data Handbook* (Springer, 2004).

45. L. Konczewicz, E. Litwin-Staszewska, M. Zajac, et al., "Electrical Transport Properties of Highly Doped N-Type GaN Materials," *Semiconductor Science and Technology* 37 (2022): 055012.

46. F. Afroz Faria, J. Guo, P. Zhao, et al., "Ultra-Low Resistance Ohmic Contacts to GaN with High Si Doping Concentrations Grown by Molecular Beam Epitaxy," *Applied Physics Letters* 101 (2012): 032109.

47. L. Lugani, M. Malinverni, S. Tirelli, et al., "n^+-GaN Grown by Ammonia Molecular Beam Epitaxy: Application to Regrown Contacts," *Applied Physics Letters* 105 (2014): 202113.

48. N. Young, R. Farrell, M. Iza, et al., "Germanium Doping of GaN by Metalorganic Chemical Vapor Deposition for Polarization Screening Applications," *Journal of Crystal Growth* 455 (2016): 105.

49. A. Ajay, J. Schörmann, M. Jiménez-Rodriguez, et al., "Ge Doping of GaN Beyond the Mott Transition," *Journal of Physics D: Applied Physics* 49 (2016): 445301.

50. P. R. Hageman, W. J. Schaff, J. Janinski, and Z. Liliental-Weber, "n-Type Doping of Wurtzite GaN With Germanium Grown With

Plasma-Assisted Molecular Beam Epitaxy," *Journal of Crystal Growth* 267 (2004): 123.

51. S. Fritze, A. Dadgar, H. Witte, et al., "High Si and Ge n-Type Doping of GaN Doping - Limits and Impact on Stress," *Applied Physics Letters* 100 (2012): 122104.

52. I. Halidou, Z. Benzarti, Z. Chine, T. Boufaden, and B. El Jani, "Heavily Silicon-Doped GaN by MOVPE," *Microelectronics Journal* 32 (2001): 137.

53. E. C. Young, B. P. Yonkee, F. Wu, et al., "Hybrid Tunnel Junction Contacts to III–Nitride Light-Emitting Diodes," *Applied Physics Express* 9 (2016): 022102.

54. K. Ueno, T. Fudetani, Y. Arakawa, A. Kobayashi, J. Ohta, and H. Fujioka, "Electron Transport Properties of Degenerate *n*-Type GaN Prepared by Pulsed Sputtering," *APL Materials* 5 (2017): 126102.

55. L. B. Rowland, K. Doverspike, and D. K. Gaskill, "Silicon Doping of GaN Using Disilane," *Applied Physics Letters* 66 (1995): 1495.

56. E. C. H. Kyle, S. W. Kaun, P. G. Burke, F. Wu, Y.-R. Wu, and J. S. Speck, "High-Electron-Mobility GaN Grown on Free-Standing GaN Templates by Ammonia-Based Molecular Beam Epitaxy," *Journal of Applied Physics* 115 (2014): 193702.

57. M. N. Fireman, G. L'Heureux, F. Wu, T. Mates, E. C. Young, and J. S. Speck, "High Germanium Doping of GaN Films by Ammonia Molecular Beam Epitaxy," *Journal of Crystal Growth* 508 (2019): 19.

58. Y.-M. Zhang, J.-F. Wang, D.-M. Cai, et al., "Growth and Doping of Bulk GaN by Hydride Vapor Phase Epitaxy," *Chinese Physics B* 29 (2020): 026104.

59. Y. Oshima, T. Yoshida, K. Watanabe, and T. Mishima, "Properties of Ge-Doped, High-Quality Bulk GaN Crystals Fabricated by Hydride Vapor Phase Epitaxy," *Journal of Crystal Growth* 312 (2010): 3569.

60. E. Richter, Ch. Hennig, U. Zeimer, L. Wang, M. Weyers, and G. Tränkle, "N-Type Doping of HVPE-Grown GaN Using Dichlorosilane," *Physica Status Solidi A* 203 (2006): 1658.

61. D. Schiavon, E. Litwin-Staszewska, R. Jakieła, S. Grzanka, and P. Perlin, "Effects of MOVPE Growth Conditions on GaN Layers Doped with Germanium," *Materials* 14 (2021): 354.

62. R. Maeda, K. Ueno, and H. Fujioka, "Pulsed Sputtering Selective Epitaxial Formation of Highly Degenerate *n*-Type GaN Ohmic Contacts for GaN HEMT Applications," *Applied Physics Express* 17 (2024): 011006.

63. X. Liu, L. Wang, D.-C. Lu, D. Wang, X. Wang, and L. Lin, "The Influence of Thickness on Properties of GaN Buffer Layer and Heavily Si-Doped GaN Grown by Metalorganic Vapor-Phase Epitaxy," *Journal of Crystal Growth* 189-190 (1998): 287.

64. R. Kirste, M. P. Hoffmann, E. Sachet, et al., "Ge Doped GaN with Controllable High Carrier Concentration for Plasmonic Applications," *Applied Physics Letters* 103 (2013): 242107.

65. S. Nakamura, T. Mukai, and M. Senoh, "Si- and Ge-Doped GaN Films Grown with GaN Buffer Layers," *Japanese Journal of Applied Physics* 31 (1992): 2883.

66. E. Lutsenko, "Gallium Nitride Opto-, Micro- and Microwave Electronics," *Science and Innovations* 1, no. 1 (2025): 22 (in Russian).

67. T. T. Mnatsakanov, M. E. Levinshtein, L. I. Pomortseva, and S. N. Yurkov, "Universal Analytical Approximation of the Carrier Mobility in Semiconductors for a Wide Range of Temperatures and Doping Densities," *Semiconductors* 38 (2004): 56.

68. N. A. Poklonski, I. I. Anikeev, E. V. Lutsenko, and S. A. Vyrko, "Data for: DC Conductivity and Mobility of a Degenerate Electron Gas in Heavily Doped GaN Crystals at Room Temperature," *Mendeley Data* (2025), https://doi.org/10.17632/j956pswzz4.

69. E. Gerlach and M. Rautenberg, "Ionized Impurity Scattering in Semiconductors," *Physica Status Solidi B* 86 (1978): 479.

70. R. P. Joshi and D. K. Ferry, "Effects of Multi-Ion Impurity Scattering on Electron Velocities in Bulk GaAs," *Semiconductor Science and Technology* 7 (1992): B319.

71. D. L. Rode and J. S. Cetnar, "Electron Mobility of Heavily Doped Semiconductors Including Multiple Scattering by Ionized Impurities," *Journal of Applied Physics* 134 (2023): 075701.